Bulletin of the Seismological Society of America, Vol. 103, No. 2A, pp. 773–786, April 2013, doi: 10.1785/0120120270

# An Earthquake Catalog for Seismic Hazard Assessment in Ecuador

by Céline Beauval, Hugo Yepes, Pablo Palacios, Monica Segovia, Alexandra Alvarado, Yvonne Font, Jorge Aguilar, Liliana Troncoso, and Sandro Vaca

**Abstract** Building a unified and homogeneous earthquake catalog is a preliminary step for estimating probabilistic seismic hazard in a country. Ecuador, a territory of ~600 km × 500 km, is characterized by an active seismicity, both in the shallow crust and in the subduction zone. Several international and local earthquake catalogs are available, covering different time and spatial windows, characterized by different magnitude types and uncertainties. After a careful analysis of each catalog, in particular for completeness and uncertainty levels, we propose a priority scheme for merging the instrumental catalogs. Moreover, several historical earthquakes are analyzed to estimate epicentral location and magnitude, completing the solutions obtained in a previous publication. Once the historical earthquakes are appended to the instrumental catalog, the resulting catalog covers five centuries in the Cordillera region. Next, homogenization of magnitudes and removal of aftershocks is performed; different options are studied and the impact on the recurrence curve is evaluated. For the Cordillera region within −2.5° and 1° latitude, the average occurrence of an earthquake with $M_w \geq 6.0$ is 10–20 years based on the historical catalog.

## Introduction

Ecuador is a seismically active country, with destructive earthquakes occurring both along the subduction zone and in the central part of the territory, in the shallow crust (see Fig. 1). The Geophysical Institute in Quito, at the Escuela Politécnica Nacional (IGEPN), is in charge of estimating the seismic hazard over the national territory. The present study is part of a broader program aimed at evaluating the probabilistic seismic hazard and producing the next seismic building code for the country. The estimation of probabilistic seismic hazard requires models of occurrence of earthquakes in time, space, and magnitude (see, e.g., Beauval and Scotti, 2003, 2004). These models rely notably on earthquake catalogs covering the longest time period possible (e.g., Braunmiller *et al.*, 2005; Grunewald and Stein, 2006; or Yadav *et al.*, 2010). In Ecuador, seismic history extends over five centuries in the Cordillera, and roughly over one century on the Coastal region (Fig. 2). The first entry in the historical database corresponds to the year 1541, shortly after the arrival of the Spaniards. Until the end of the nineteenth century, the historical information mostly describes effects of earthquakes in the Cordillera. The first coastal event for which several intensities are reported is in 1896 (Fig. 2).

Since the beginning of the 1990s, there have been a few studies aimed at developing earthquake catalogs at the scale of the Northern Andes (e.g., Dimate *et al.*, 1999; Giesecke *et al.*, 2004). The objective of this new study is to focus on Ecuador and the surrounding area, to take into account the revised IGEPN local catalog, the recently improved characterization of historical earthquakes (Beauval *et al.*, 2010), and the overall improved localization of earthquakes at the international scale (e.g., Engdhal and Villaseñor, 2002; and the updated "EHB" catalog, ISC, 2010). The spatial window considered here covers a region that extends in latitude from −7° to +4° and in longitude from −84° to −74° (roughly 1100 × 1000 km; Fig. 1). This spatial window encloses all seismic sources able to generate significant ground motions in the Ecuadorian territory. In the first part of this paper we detail the process of building the earthquake catalog: analysis of the available information sources, schemes to merge the different instrumental catalogs, tests to homogenize the magnitude, and extension of the historical catalog with new analysis of several past earthquakes. In the second part, we focus on the Cordillera region. The analysis of the unified catalog, completeness issues, and removal of short-term clustered events enable us to derive frequency–magnitude distributions. Recurrence times for significant earthquakes are determined for the Cordillera region.

## A Homogeneous Earthquake Catalog

### Instrumental Earthquake Catalogs

Ecuador's seismicity can be studied through international and local catalogs (Tables 1 and 2; Fig. 2). The Ecuadorian seismic network (RENSIG) is run by the Geophysical Institute in Quito. The local catalog (IGEPN) provides earthquake solutions for the time period 1990–present. The reported

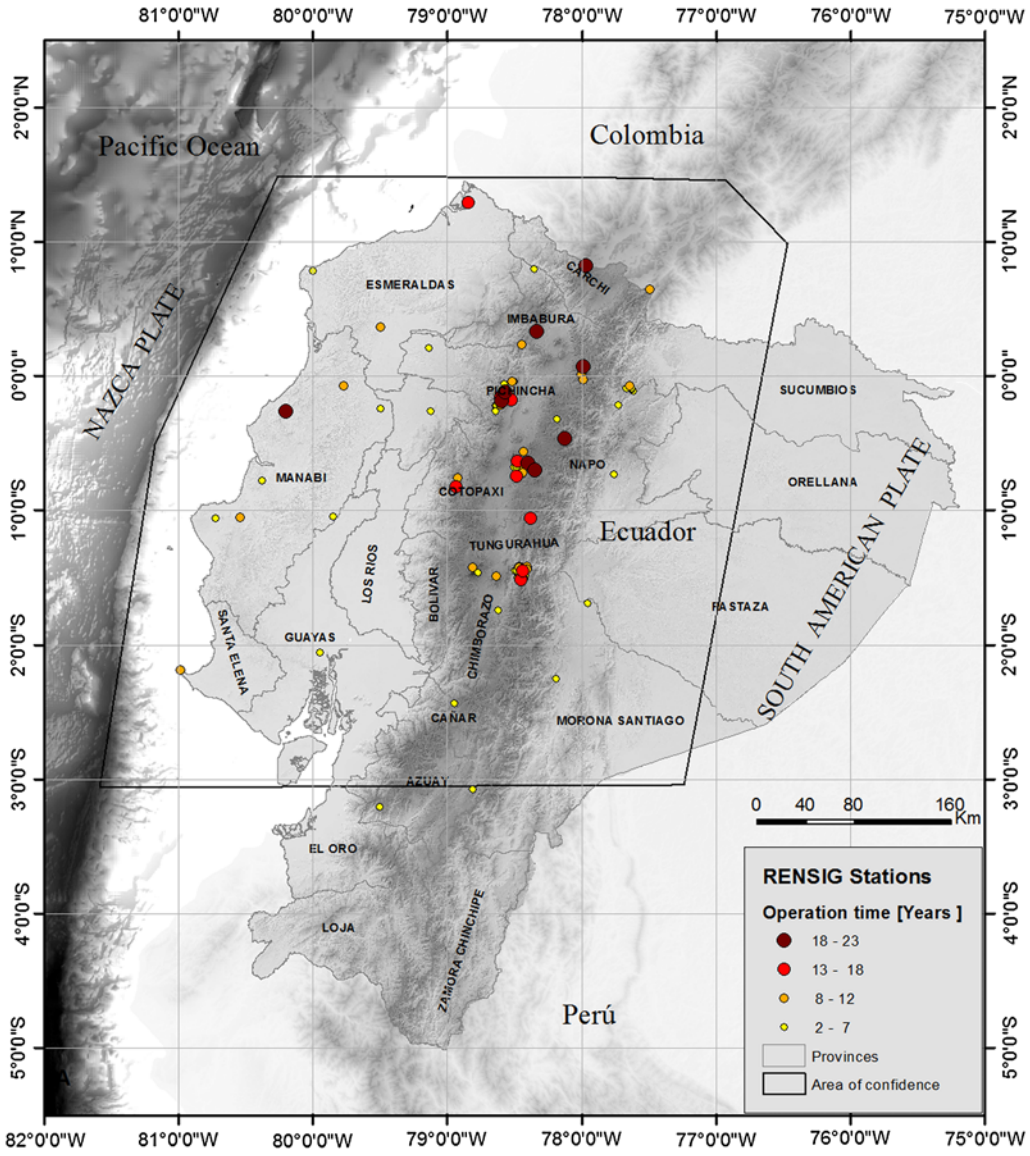


**Figure 1.** IGEPN seismological network, circles. Radius of circle: operation times of stations. Area of confidence for the IGEPN network, polygon (see text). Province names are indicated. The color version of this figure is available only in the electronic edition.

magnitude is duration magnitude ($M_D$) calculated on the Coda waves (Palacios and Yepes, 2011). The RENSIG stations guarantee reliable solutions inside a spatial window that encompasses the area identified by the polygon in Figure 1. Within this zone, the network exhaustively records events with magnitudes down to $\sim M_D = 3.5$. As Font *et al.* (2013) have been working on improving the locations of the IGEPN events, their locations are preferred to IGEPN locations when they exist. For the rest of the country, southern Ecuador and the Amazonia to the East, the IGEPN solutions are not reliable and are not included in the catalog. In these zones, the international catalogs National Earthquake Information Center Preliminary Determination of Epicenters (NEIC-PDE from the U.S. Geological Survey) and International Seismological Centre (ISC) provide more accurate solutions than the RENSIG, though with a higher completeness magnitude (body-wave magnitude, $m_b = 4.5$). Note that RENSIG has evolved considerably since 2010, as more stations have been installed and the network now homogeneously covers the territory. The local catalog's completeness in space and in magnitude will be greatly improved over the next years.

The ISC catalog reports solutions beginning in 1900 (International Seismological Summary [ISS]) and its own solutions since 1964; the NEIC-PDE catalog is providing solutions for earthquakes beginning in 1963 (see, e.g., Johnston and Halchuk, 1993, who provide some useful information on the history of these catalogs). Moreover, three other catalogs are worth integrating into our study, as they contain events with magnitudes usually larger than ~5.5. The first one is the Centennial catalog compiled by Engdhal and Villaseñor (2002) covering the twentieth century, for which earthquakes are relocated using the Engdahl *et al.* (1998) method. They

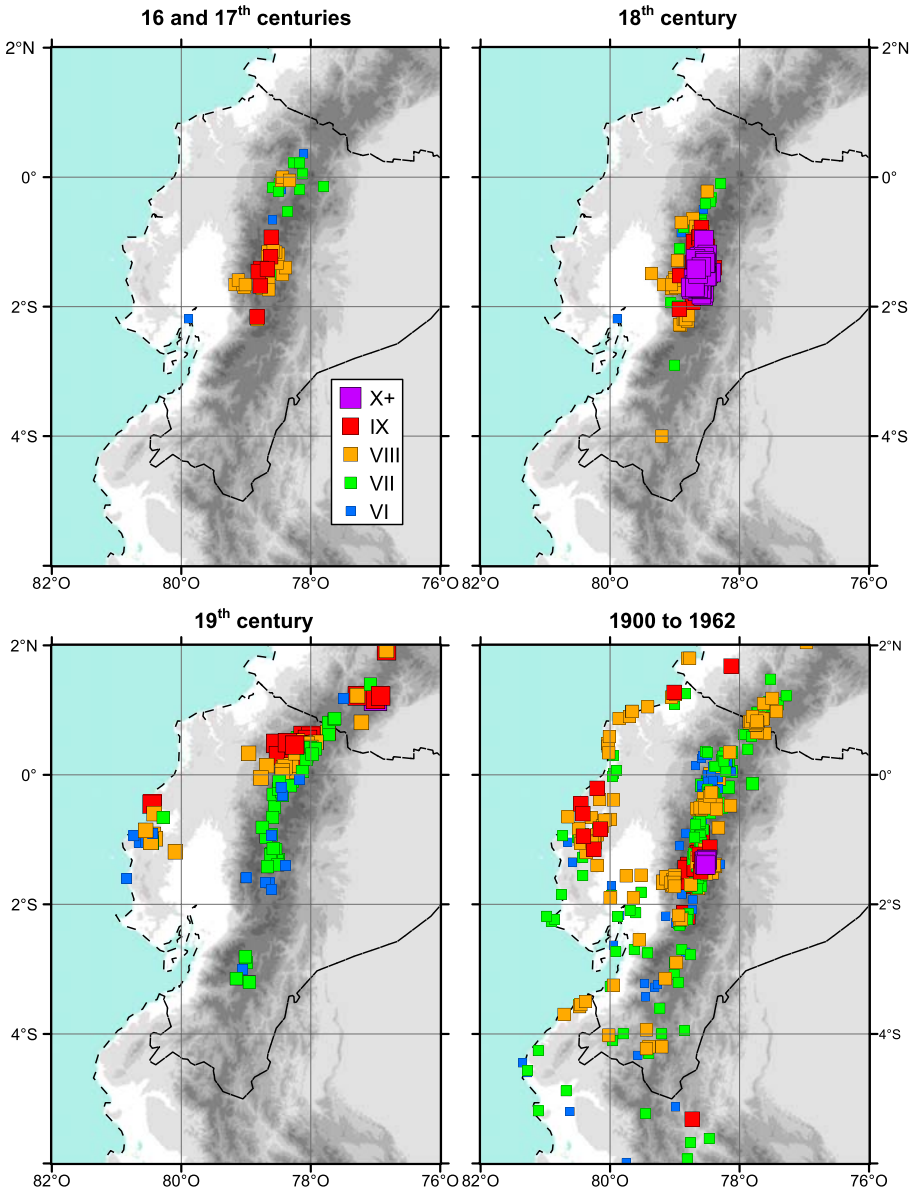


**Figure 2.** Intensity database for Ecuador (Egred, 2009), containing events with at least one intensity VI reported. All individual intensity assignments are plotted on the maps, considering all earthquakes reported in the database. First information for coastal events at the end of the nineteenth century. The color version of this figure is available only in the electronic edition.

report existing magnitude estimates (with a priority order, see p. 667 of their paper). The second catalog is the EHB-ISC catalog (2009), a refined version of the ISC catalog. From 1960 until 2009, Engdahl *et al.*'s (1998) algorithm has been used to significantly improve routine hypocenter determinations made by the ISS, ISC, and PDE. Last, another international catalog worth considering is the Global Centroid Moment Tensor catalog (GCMT; Ekström *et al.*, 2012), which since 1976 has been reporting moment magnitude ($M_w$) for some moderate-to-large events all over the world. The time periods covered by each catalog and the magnitude types reported are described in Tables 1 and 2 and Figure 3. Note that for four major subduction earthquakes, the 1906 ($M_w$ 8.8), 1942 ($M_w$ 7.8), 1958 ($M_w$ 7.8), and 1979 ($M_w$ 8.1) events, with fault planes extending over hundreds of kilometers, the epicenter coordinates are extracted from specific studies (for the 1906 event: Swenson and Beck, 1996; for the other three events: Mendoza and Dewey, 1984).

## Merging Different Instrumental Earthquake Catalogs

The first step toward building a unique and homogeneous catalog for the country consists of identifying the same events in the different catalogs. This task can be difficult as there might be uncertainties or lack of entries in the time, magnitude, coordinates, and depth of the solutions. Several tests were performed, which are not detailed here, to understand the uncertainties associated to each catalog and to produce a master catalog with all available solutions

Table 1
Earthquake Catalogs Used for Magnitude Selection in Descending Priority Order

| Catalog | Covered Time Period | Magnitude Type |
|---|---|---|
| GCMT/HRV | 1976–2009 | $M_w$ |
| Centennial | 1900–2001 | Unknown, $m_B$, $m_b$, $M_S$, $M_w$ |
| ISC, determined by BRK, PAS | 1900–1963 | $M_S$ and unknown |
| ISC, determined by ISC | 1964–2009 | $m_b$ from 1964<br>$M_S$ from 1978 |
| NEIC, determined by USGS-NEIC | 1963–2010 | $m_b$ from 1963<br>$M_S$ from 1968<br>$M_w$ from 1982 |
| IGEPN | 1997–2009 | $M_D$ |

Table 2
Earthquake Catalogs Used for Location Selection (see Fig. 3)

| Catalog | Time Period | Spatial Area of Confidence |
|---|---|---|
| IGEPN-FONT | 1994–2007 | See Figure 1 |
| IGEPN | 1993–2009 | See Figure 1 |
| EHB (in the ISC) | 1960–2007 | The whole window |
| Centennial | 1900–2001 | The whole window |
| ISC, determined by ISS/GUTE | 1900–1962 | The whole window |
| ISC, determined by ISC | 1964–2009 | The whole window |
| NEIC, determined by USGS-NEIC | 1963–2009 | The whole window |

The spatial window considered is in latitude −7° to 4.0°, in longitude −84° to −74°.

listed per event. All events reported by different catalogs, separated by <2 minutes in time and 100 km in distance, have been manually checked. International catalogs are used only for magnitudes 4.0 and above, which limits the number of events to be checked manually and the problems of mistakenly associating earthquakes. Then, a hierarchy is required for the selection of the location and for the selection of the magnitude for each event in the master catalog (Fig. 3).

This study develops a proxy for a moment-magnitude catalog of earthquakes in which the selection of the magnitude is as follows, by decreasing priority order: $M_w > M_S > m_b > M_D$ (Table 1, Fig. 3). Inside the spatial window considered, only 242 events of the master catalog have moment magnitude directly calculated by the GCMT/HRV. From 1964 on, most events with a magnitude ≥4.5 have $m_b$ (body-wave magnitude) determined by the ISC. A surface-wave magnitude $M_S$ is selected prior to $m_b$ whenever $M_S$ exists and is >5.5, as $m_b$ saturates around 5.8–6.0 (e.g., Utsu, 2002). The magnitude $M_D$ calculated by the IGEPN is based on an equation calibrated on $m_b$. Note that $M_D$ is not reliable before 1997 (Palacios and Yepes, 2011); therefore, events occurring before that year described by a unique magnitude $M_D$ are not taken into account.

The selection of the preferred location depends on the location of the event. If the earthquake is located inside the area of confidence of the RENSIG network (Fig. 1), the IGEPN/FONT solution is considered the best solution, the second-best solution being the original IGEPN one. Even though RENSIG has been running since 1990, it was not until 1993 that hypocentral solutions were calculated using verifiable standards. If the earthquake falls outside this area of confidence, or if the earthquake occurred before 1993, the location solution is selected from solutions provided by international networks. In this case, the priority order that has been used is EHB > Centennial > ISC > NEIC (Table 2, Fig. 3). The EHB solutions (ISC, 2010) are the most recent solutions obtained applying the Engdhal *et al.* (1998) relocalization technique. Moreover, as the ISC usually uses the greatest number of stations, its location is preferred over the NEIC solution.

Earthquakes in the catalog have minimum magnitudes greater or equal to 3.0 ($M_D$), as the completeness of smaller magnitudes is highly space dependent, and thus they cannot be used in the development of recurrence models. Events with magnitudes lower than $m_b = 4$ outside the RENSIG window of confidence are likewise excluded. Neither the RENSIG network nor the international networks are able to determine reliable solutions for such events. The final catalog, containing for each event the best solutions in magnitude and in location, has 10,823 events. As indicated in Table 3, the majority of these events are described by an $M_D$ (7541). This proportion drops if considering higher minimum magnitude threshold (165 events out of 3139 for $M4+$, and 10 out of 1639 for $M4.5+$). Approximately 70% of the earthquakes with $M \geq 4$ are described by an $m_b$ as calculated by the ISC.

### Homogenization of Magnitudes to Moment Magnitude

The entire set of earthquakes in the catalog must be characterized by $M_w$ or an equivalent $M_w$, as the recent ground-motion prediction equations are in terms of $M_w$. To homogenize magnitude in a catalog, different techniques may be considered. The obtained catalog contains 68 events for the period prior to 1963, described with varied magnitude types (unknown, $m_B$, $M_S$, $M_w$,) and authors (see Engdhal and Villaseñor, 2002). Using the Centennial catalog, Engdhal and Villaseñor (2002) conclude that magnitude estimates listed by Abe (1981, 1984; ABE $M_S$) and by Pacheco and Sykes (1992; P&S $M_w$) are consistent with GCMT/Harvard $M_w$ estimates. Furthermore, they demonstrate that magnitudes reported by Gutenberg and Richter (1954, G&R), Rothé (1969, ROTHE), and Pasadena (PAS) before 1960, are systematically larger than Abe (1981) $M_S$ by 0.2 magnitude units on average. Thus, a 0.2 magnitude unit reduction is applied on the magnitudes with sources G&R, ROTHE, and PAS of our catalog.

The magnitudes of earthquakes belonging to the more recent part of the catalog, from 1963 on are (1) body-wave magnitude $m_b$ calculated by either the ISC or the NEIC-PDE, (2) duration magnitude $M_D$ estimated by the IGEPN, (3) surface-wave magnitudes $M_S$, calculated by either the ISC or

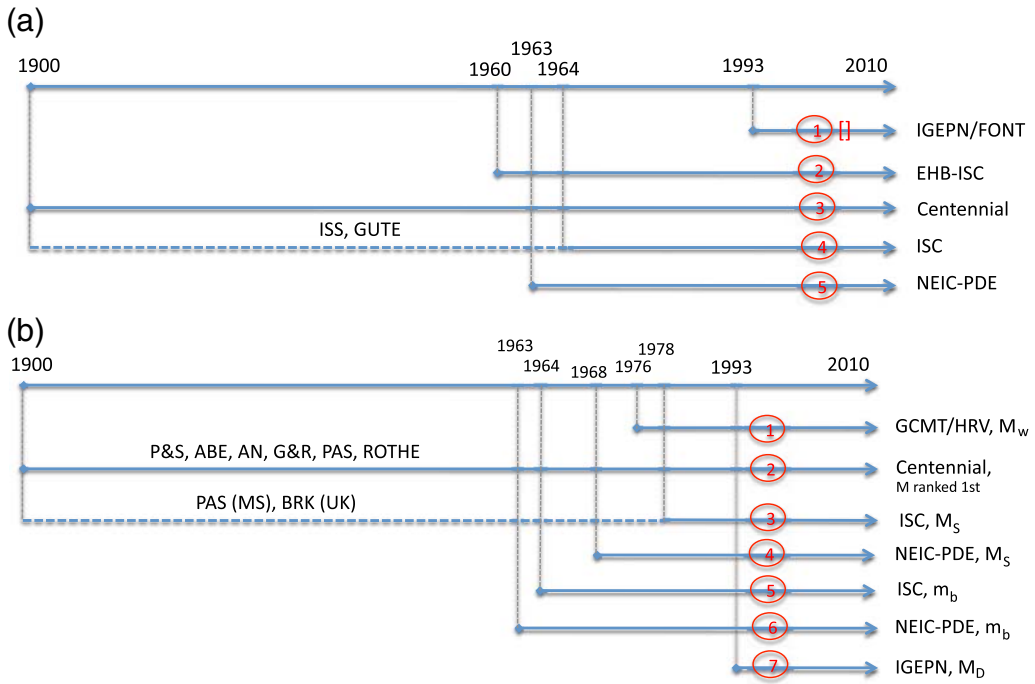


**Figure 3.** (a) Prioritized list for assigning the preferred location for an event of the master catalog. Time periods covered by each catalog are indicated. The IGEPN/FONT is the only catalog used on a restricted spatial window (see Fig. 1). (b) Prioritized list for assigning the preferred magnitude. Magnitude types are specified. See the text for abbreviations. Note: if the magnitude reported in the Centennial catalog has been calculated by the ISC, it is taken directly from the ISC catalog. The color version of this figure is available only in the electronic edition.

the NEIC-PDE, and (4) moment magnitude $M_w$ determined by GCMT/Harvard. The data used to establish an equation of magnitude conversion usually show that dispersion can be large (e.g., Scordilis, 2006) and that applying an equation may have a great impact on a catalog. Our practice in the current work is to use a conversion equation only when it is considered mandatory. Among others, Utsu (2002) has shown that magnitudes $m_b$ and $M_S$ can be considered approximately equivalent to $M_w$ for magnitudes $m_b$ up to 6.0 and magnitudes $M_S$ up to 8.0, respectively (fig. 1 in Utsu, 2002). At first, we decide to use magnitudes $m_b$ and $M_S$ as surrogates for $M_w$ in the appropriate magnitude ranges.

For earthquakes with low magnitudes, usually only a local $M_D$ is available. The $M_D$ is calculated using an equation calibrated on magnitudes $m_b$ (Palacios and Yepes, 2011). In Figure 4, the $m_{b_{ISC}}$ magnitude is plotted against the corresponding $M_D$, for all events described by both magnitude types. $M_D$ shows to be on average equivalent to $m_{b_{ISC}}$, with some dispersion. Plotting the difference between both magnitude estimates versus time (Fig. 5), the difference proves to be centered on zero and rather stable with time. Therefore, we also consider $M_D$ to be a reasonable surrogate for $M_w$. This option is called the surrogate option.

A second option consists of applying empirical conversion relationships. For this purpose, the relations between different magnitude types in the region of interest need to be studied. The relations between magnitudes $m_{b_{ISC}}$ and $m_{b_{NEIC}}$, and between $m_{b_{ISC}}$ and $M_{w_{GCMT}}$, must be analyzed (Fig. 6). We show that $m_{b_{ISC}}$ is approximately equivalent to $m_{b_{NEIC}}$ (using 2218 events in the spatial window considered). Scordilis (2006), based on worldwide data, came to the same conclusion. Furthermore, we propose the following relation between magnitudes $m_{b_{ISC}}$ and $M_{w_{GCMT}}$ (valid for the interval 4.5–6 in the considered spatial window; Fig. 6):

$$M_{w_{GCMT}} = 0.93 m_{b_{ISC}} + 0.6. \quad (1)$$

This equation is close to the equation derived by Scordilis (2006), using data on a global scale ($M_{w_{GCMT}} = 0.85$

Table 3
Number of Earthquakes in the Final Unified Instrumental Catalog
(Surrogate Option)

| Number of Events 1901–2009 | In Total | With $M_D$ | With $m_b$ (ISC) | With $m_b$ (NEIC) | With $M_S$ (ISC or NEIC) | With $M_w$ (GCMT) |
|---|---|---|---|---|---|---|
| *M*3+ | 10,823 | 7541 | 2580 | 365 | 16 | 242 |
| *M*4+ | 3139 | 165 | 2296 | 343 | 14 | 242 |
| *M*4.5+ | 1639 | 10 | 1160 | 135 | 13 | 242 |

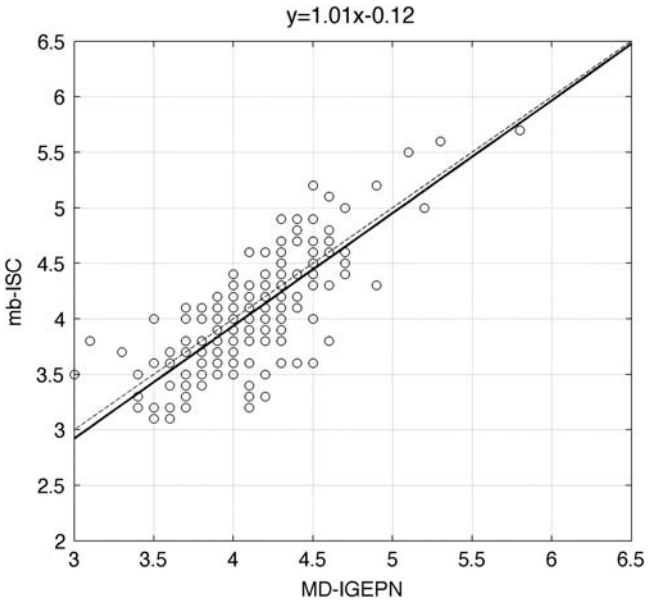


**Figure 4.** Correlation between $m_b$ (ISC) and $M_D$ (IGEPN): from 201 earthquakes described by both magnitudes types ($M_D$ [IGEPN] $\geq$3 and $m_b$ [ISC] $\leq$5.8), in the spatial window with latitudes from −3° to 1° and with longitudes from −80° to −77.5°.

$m_{b_{ISC/NEIC}} + 1.03$; see p. 231, Scordilis, 2006). For the homogenized catalog option, all $m_b$ as well as local $M_D$ are converted into an equivalent $M_w$ using equation (1). The equation is valid only on the magnitude interval of the generating data set, that is to say, for magnitudes $m_b$ above 4.5 (Fig. 6). Applying the equation to the whole catalog, the equation is extrapolated toward lower magnitudes (down to $M_D$ 3.0). Magnitudes concerned are $M_D$ between 3.0 and 4.5, resulting in $M_w$ between 3.4 and 4.8. Moreover, to check the dependence of equation (1) with the depth of earthquakes, two equations were derived separately considering events with depths below and above 40 km (respectively, 107 and 103 events). The equations obtained were close to equation (1), and we decided not to include a depth dependence in this conversion equation.

Uncertainties and hypothesis underlie both options of building the final catalog. In the section on the Recurrence Times of Earthquakes in the Cordillera, we illustrate the impact on the seismicity rates of choosing one option or the other.

## The Historical Catalog

In a previous work, Beauval *et al.* (2010) analyzed the intensity database of Egred (2009) and derived locations and magnitudes for nineteen historical earthquakes (1587–1976, $5.0 \leq M_w \leq 7.6$; tables 4 and 5 in Beauval *et al.*, 2010). The Bakun and Wentworth (1997; B&W) methodology was applied to provide locations and magnitudes with associated uncertainties. Many events in the intensity database were left aside, as their intensity data sets did not allow the application of the B&W method. These data sets are either too small or are made of only one or two intensity degrees. In the present study, the earthquake catalog is built for seismic hazard purposes, and it must be as complete as possible. These earthquakes must be analyzed, and ways to evaluate potential locations and magnitudes are needed. These solutions will bear large uncertainties that must be evaluated. Note that aftershocks are not taken into account (e.g., the 27 December 1926 event, which is an aftershock of the 18 December 1926 event on the El Angel–Guachucal fault system at the Colombian border).

For each of the earthquakes listed in Table 4, the distribution of the intensities in space has been checked and the potential responsible fault has been identified based on tectonic arguments (Alvarado, 2012). The preferred epicentral location is selected on the fault. The magnitudes corresponding to different locations on the fault are obtained by simply calculating the mean value of all magnitude values inferred from the individual intensity assignments (as done in the B&W method; see equation 3 in Beauval *et al.*, 2010).

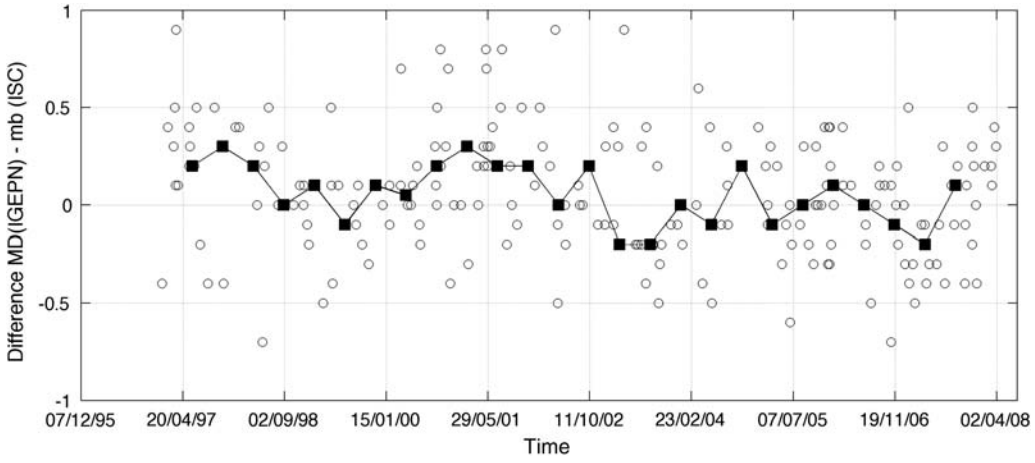


**Figure 5.** Differences between $M_D$ calculated by the IGEPN, and $m_b$ calculated by the ISC, for all earthquakes with $M_D$ (IGEPN) $\geq$3 and $m_b$ (ISC) $\leq$5.8 described by both magnitudes types, in the spatial window with latitudes from −3° to 1° and with longitudes from −80° to −77.5°. Differences are plotted against time to check the stability of the duration magnitude determination with time. Mean differences calculated in sliding time windows, squares.

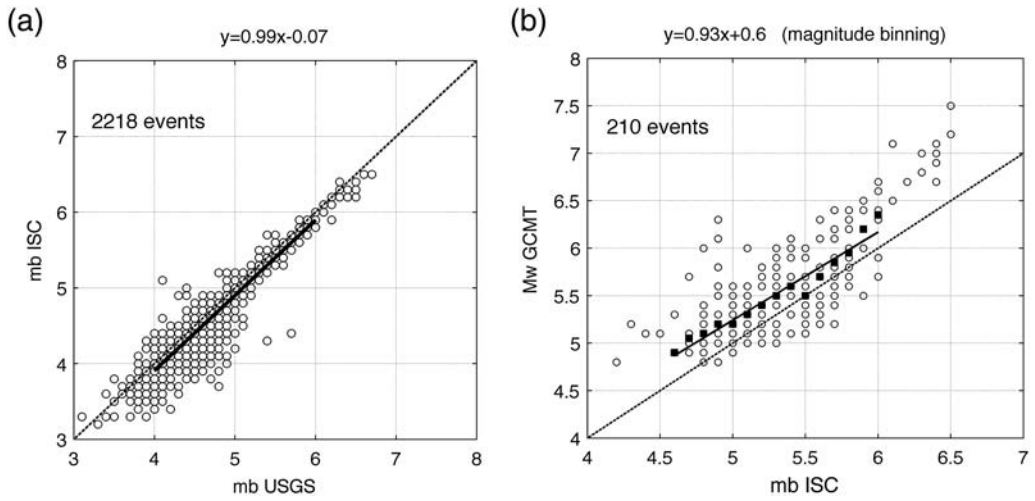


**Figure 6.** (a) Correlation between $m_b$ (ISC) and $m_b$ (NEIC/UGSG), considering all earthquakes described by both magnitude types in the spatial window within latitudes from −6° to +3.0° and longitudes from −83° to −75°. The thick segment is the conversion equation obtained from $4 < m_b(\text{NEIC}) < 6$. (b) Correlation between $M_w$ (GCMT) and $m_b$ (ISC), considering all earthquakes in the magnitude range [4.6; 6.0], in the spatial window with latitude −6° to +3°, longitude −83° to −75°. The regression is performed after applying a magnitude binning (0.1-unit $m_b$-bins).

Magnitudes from individual intensities are estimated using the attenuation equation established for the Cordillera region in Beauval *et al.* (2010; equation 2). In the B&W technique, the uncertainty in the magnitude and location estimates is inferred from bootstrapping on the intensity data set. The data sets considered here are very small, and the bootstrapping technique would not give meaningful results.

We adopt another strategy for taking into account the uncertainty on the intensity data set. For previous centuries, when all structures were made of adobe, there has always been doubt of assigned intensities higher than VIII, as intensity descriptions may "saturate" at VIII. In the Andes, all colonial structures such as churches and towers where built either with adobe bricks, mud walls, or stones, with heavy tile roofs. These are vulnerability type A structures in the EMS-98 intensity scale (Grünthal, 1998). Grade 4 (very severe) or grade 5 (total destruction) damages in type A structures should be described with intensity VIII. Before detailed intensity descriptions in scales like EMS-98, widespread destruction during colonial earthquakes has been related to higher intensities. In Beauval *et al.* (2010), tests have been led for various events to check that the highest intensity degrees were not biasing the results. Considering the present earthquakes with much smaller data sets, where only upper intensity degrees are available, such tests cannot be done. The strategy we adopt for taking into account the uncertainty on the available intensity sample is as follows: two calculations are performed, one based on the original intensity set, and the other one on a data set made of these intensities decreased by one degree. The ranges obtained for the magnitude are large (Table 4), but we believe that they are representative of the true uncertainty. Solutions are obtained for thirteen earthquakes located in the Cordillera, from 1645 until 1953, with magnitude estimates ranging from 5.7 to 7.6.

To further improve the magnitude and location estimates for these earthquakes, a thorough historical work will be required, which includes reviewing the archives for more information. Around 20 earthquakes with maximum intensity VII or VIII in the intensity database are still not included (e.g., in 1541, 1557, 1575…). They are described by less than five intensities, and there is currently not enough information to propose a responsible fault and derive earthquake parameters. Finally, some work is required in the future to also provide solutions for the two historical earthquakes that affected the coast (3 May 1896 and 17 April 1898, Manabí province).

## Final Unified Earthquake Catalog

The unified earthquake catalog 1587–2009 integrates instrumental and historical earthquakes, from magnitude 3 and above. It comprises 10,823 instrumental events plus 32 historical earthquakes. As expected, the seismicity distribution reflects the two major tectonic features in the country: the subduction of the Nazca plate and the active crustal deformation occurring in the Andean Cordillera (Fig. 7).

Regarding the subduction zone, the largest earthquakes are concentrated north of ∼1° S. The two $M_w > 8$ earthquakes present in the catalog are related to this segment of the subduction zone. In this zone, the seismogenic part of the interface extends over 120 km from the trench, penetrating ∼50 km inland. Almost no earthquakes deeper than 120 km are found farther east. South of 2° S, the distribution of the subduction seismicity is not clear, and earthquakes in the depth range 40–120 km are distributed almost uniformly regardless of the physiographic region or the distance from the trench. Significant earthquakes $M_w$ 7–8 are concentrated in the southwestern portion of the Guayaquil Gulf area around 4° S. These two dissimilar patterns in the seismicity

Table 4
Historical Earthquakes Analyzed in This Study

| yyyy/mm/dd | Epicentral Region (Fig. 1) | IV | V | VI | VII | VIII | IX | X | XI | Fault or Fault System* | Preferred Location of Epicenter† | $M_w$‡ |
|---|---|---|---|---|---|---|---|---|---|---|---|---|
| 1645/03/15 | Chimborazo | 1 | — | — | 3 | 2 | 1 | — | — | Pallatanga | −1.73; −78.8 | 6.7–7.3 |
| 1674/08/29 | Bolivar | — | — | — | — | 7 | — | — | — | San Jose de Chimbo | −1.67; −79.05 | 6.1–6.8 |
| 1687/11/22 | Tungurahua | — | — | 1 | 4 | 5 | — | — | — | Pucara | −1.25; −78.42 | 5.9–6.6 |
| 1736/12/06 | Cotopaxi | — | — | 1 | 5 | 1 | — | — | — | Saquisili-Poalo-Yambo (SPY) | −0.75; −78.75 | 5.7–6.2 |
| 1757/02/22 | Latacunga | — | 1 | 1 | 4 | 3 | — | — | — | SPY | −0.92; −78.56 | 5.9–6.4 |
| 1786/05/10 | Chimborazo | — | — | — | 9 | 4 | — | — | — | Pallatanga | −1.68; −78.78 | 5.4–6.2 |
| 1834/01/20 | Carchi/Nariño | 2 | 1 | — | 2 | 3 | 5 | 1 | 1 | Sibundoy | 1.12; −77.00 | 7.2–7.6 |
| 1868/05/17 | Tungurahua | — | — | 1 | 8 | — | — | — | — | Pucara | −1.25; −78.42 | 5.7–6.7 |
| 1923/02/05 | Pichincha | — | — | — | 2 | 6 | — | — | — | Machachi | −0.55; −78.63 | 5.8–6.5 |
| 1923/12/14 | Carchi/Nariño | 1 | 1 | 3 | 8 | 12 | — | — | — | El Angel-Guachucal | 0.88; −77.8 | 5.8–6.5 |
| 1926/12/18 | Carchi/Nariño | 2 | — | 1 | 4 | 3 | — | — | — | El Angel-Guachucal | 0.87; −77.78 | 5.7–6.4 |
| 1953/12/23 | Carchi/Nariño | — | 4 | 5 | 6 | — | — | — | — | Guaitara | 1.05; −77.36 | 5.7–6.3 |

Intensity data, potential responsible fault, location, and equivalent moment magnitude deduced from the magnitude isocontours.
*Potential responsible fault (see Beauval *et al.*, 2010, in particular Table 6).
†Preferred epicenter location selected on the responsible fault.
‡Interval of uncertainty for the magnitude.

distribution are related to the differences in dip of the Nazca plate; the downgoing slab has a shallower dip in the south. There is a concentration of deeper earthquakes (depth > 120 km) around latitude 1.5° S and longitude 78° W known as the Puyo seismic cluster. These are intraslab events with moderate magnitudes clustered in space (but not in time). Within this cluster, the largest known recorded magnitude occurred outside the time window analyzed in the present work ($M_w$ 7.2 in 2010). Their focal mechanisms reflect tearing of the subducting slab with strike ~N45°W (Segovia and Alvarado, 2009).

The crustal seismicity along the Cordillera also shows two different patterns north and south of 2° S (Fig. 7). Along the southern latitudes, to the east, a northwest–southeast trend of moderate $M_w$ 6–7 events with large $M_w$ 7–7.5 earthquakes is clear along the Andean foothills in the Amazon basin in northwestern Peru. This trend is parallel to the direction of the Andean Cordillera and could be related to its active growth to the east. North of 2° S, the seismicity is concentrated in the Cordillera and shows shallow depths in relationship with the deformation of the North-Andean block (Alvarado, 2012). Most of the historical events are located in this region, and five of them show large magnitudes $M_w$ 7–7.6. Instrumental events are also shallow and have similar epicentral distribution along the Andean Cordillera in agreement with locations of historical events, therefore adequately reflecting the seismic potential in Ecuador.

## Recurrence Times of Earthquakes in the Cordillera

### Declustering of the Catalog

From Christophersen *et al.* (2011, p. 2): "Declustering, i.e., the removal of earthquakes that occur in clusters such as aftershock sequences and swarms, is not an exact science, as no physical difference are known to exist between foreshocks, mainshocks, and aftershocks. Therefore, earthquake clusters are usually defined by their proximity in time and space." Keeping this in mind, clustered events need nonetheless to be retrieved from the earthquake catalog, so that the recurrence curves reflect the occurrences of earthquakes related to the regional tectonics and are not biased by overestimated low-magnitude rates. As in many seismic hazard studies, the catalog is declustered using Reasenberg's (1985) algorithm. Reasenberg's (1985) code is known as a "linking" algorithm, where clusters are linked by smaller earthquakes and are allowed to grow in time and space (for more details, see Lolli and Gasperini, 2003; Christophersen and Smith, 2008). In brief, the time interaction window is based on the Omori decay for aftershock activity, whereas the spatial interaction zone depends on the magnitude of prior events. Its extension is inferred from the stress redistribution around the most recent and the largest earthquakes in the sequence.

The impact on the declustering of the calibrating parameters is analyzed through a simple sensitivity study based on the surrogate earthquake catalog. Three parameters constraining spatial and time interaction zones are considered: the minimum and maximum look-ahead time $\tau_{min}$ and $\tau_{max}$, and the factor for the spatial interaction distance $r_{fact}$. The minimum look-ahead time is used in the case of earthquakes not already associated to a cluster. Note that the location errors of earthquakes are taken into account by fixing the horizontal and vertical errors to 10 km until 1992, and 5 km from 1993 on. Table 5 displays the percentage of aftershocks identified in the catalog, modifying one by one the three parameters. The first set of parameters ($\tau_{min} = 2$, $\tau_{max} = 10$, $r_{fact} = 10$) corresponds to the default parameters in Reasenberg's (1985) code. The minimum and maximum look-ahead times are extended up to 10 and 20 days, respectively, whereas the distance factor is increased to 15. The

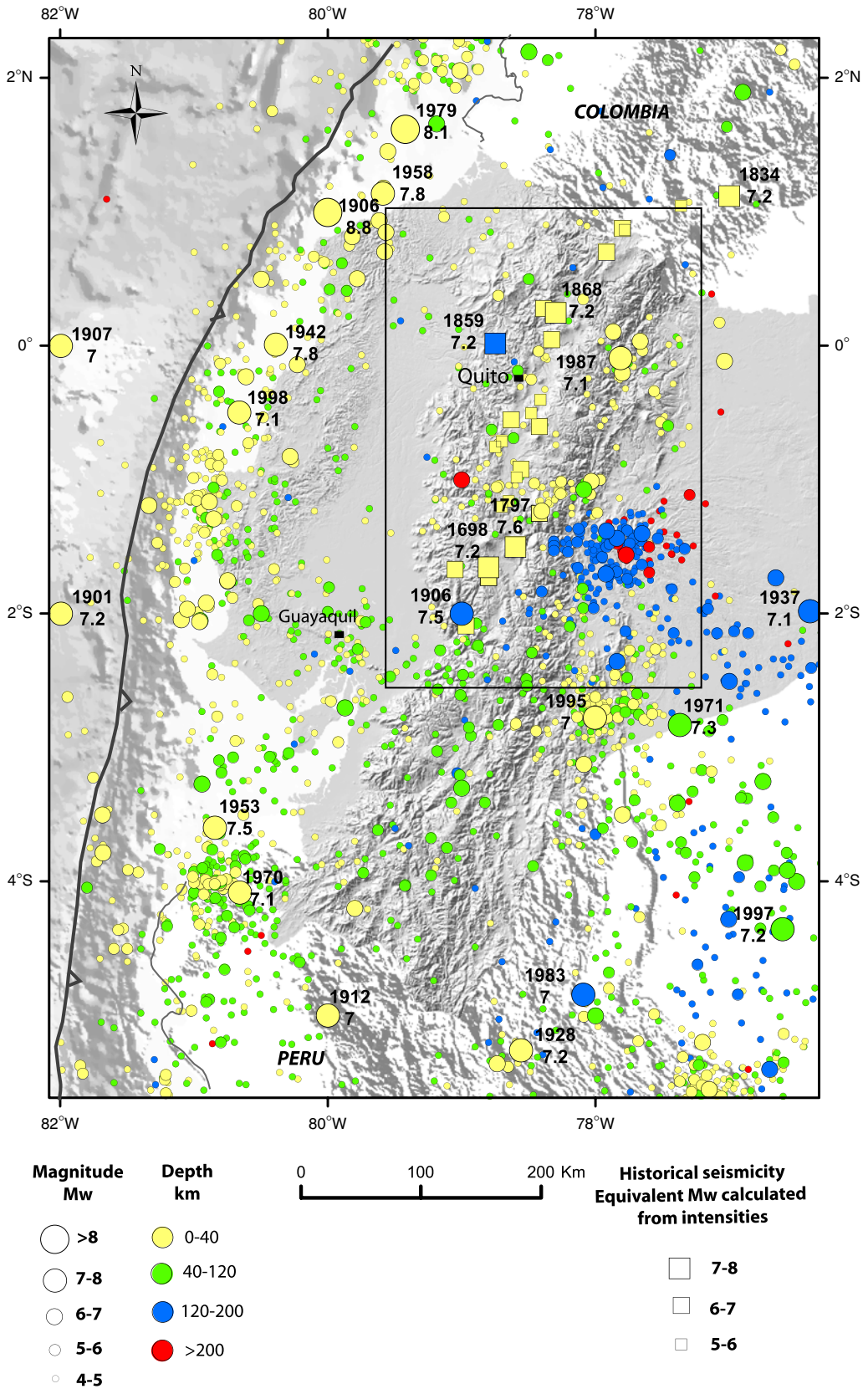


**Figure 7.** Epicenters from the unified earthquake catalog 1587–2009, integrating instrumental and historical earthquakes, displaying magnitude 4 and above (surrogate option, see the text). The recurrence is estimated for crustal earthquakes within a zone focused on the Cordillera (rectangle). Year of occurrence and magnitude are indicated for earthquake with $M_w \geq 7.0$. The color version of this figure is available only in the electronic edition.

Table 5
Five Parameters Combinations, Used for Applying the Reasenberg (1985) Declustering Algorithm on the Earthquake Catalogue (Surrogate Option)

| $\tau_{min}$ (days) | $\tau_{max}$ (days) | $r_{fact}$ | % Aftershocks |
|---|---|---|---|
| 2 | 10 | 10 | 21 |
| 2 | 20 | 10 | 24 |
| 4 | 20 | 10 | 26 |
| 4 | 20 | 15 | 27 |
| 10 | 20 | 15 | 32 |

$r_{fact}$ is a multiple of the circular crack radius.

percentage of aftershocks identified in the Ecuadorian catalog varies between 21% and 32%. We have checked on well-identified sequences (such as the 1996 Pujilí event or the 1987 Salado–Reventador events) that the declustering procedure correctly identifies clustered events. In the following, a recurrence curve is obtained for the Cordillera based on the five declustered catalogs, showing very little impact of using one or the other declustered earthquake catalog. The declustered catalog selected as reference is the one obtained after removing 32% of clustered events. Applying the same set of parameters on the catalog homogenized in magnitude leads to a reduction of 33% of the total number of earthquakes.

## Recurrence Times of Potentially Destructive Earthquakes in the Cordillera

Based on the declustered earthquake catalog, mean recurrence times can be estimated for earthquakes with given magnitudes. Because of the history of settlements and a climate favorable to document conservation, the information on past earthquakes extends over a longer time window in the Cordillera than in other parts of the country (five centuries; Fig. 2). Moreover, until very recently most stations of the local network were installed mainly on the active volcanoes within the Cordillera (Fig. 1). Therefore, the completeness in the recording of earthquakes is best within the Cordillera. Average recurrence times for significant earthquakes within the volcanic chain, between latitudes −2.5° and +1° are determined (see Fig. 7 for the area considered). Several cities with large populations, among them the capital Quito, are located in this area.

To establish a recurrence curve, seismic rates need to be calculated over the complete periods of the catalog. Time periods of completeness are determined from the classical plots displaying cumulated number of events versus time, for different magnitude intervals (four intervals are displayed in Fig. 8). The most recent linear segment, indicating a stable seismic rate with time, provides the lower bound of a completeness period. The plots are displayed for the two optional earthquake catalogs, one based on the surrogate assumption and the other resulting from applying magnitude conversion equations (see Homogenization of Magnitudes to Moment Magnitude). Based on Figure 8, the same set of completeness time windows is selected for both catalogs (Table 6 and Fig. 9). As in most hazard studies in any part of the world, identifying complete time periods is not an easy task; none of the plots in Figure 8 shows a perfect linear segment. The dates selected based on the cumulated number of events, however, also correspond to meaningful key dates in the development of seismological networks: 1997 is the beginning date for the IGEPN catalog we are using, whereas 1963 marks the beginning of international seismological networks.

Finally, from the observed rates, the Gutenberg–Richter parameters are calculated (Weichert, 1980) and the recurrence curve is modeled (Figs. 10 and 11). Initially, the recurrence is modeled for the five optional declustered catalogs (see Table 5 and Declustering of the Catalog). The Gutenberg–Richter parameters do not vary much depending on the declustered catalog considered (Fig. 10). Note that if considering smaller source zones, as will be done in the probabilistic seismic hazard calculations, the impact on the recurrence curve might be more significant. From now on, the catalog that is used is the catalog resulting from the removal of 32% of the clustered events (33% in the case of the homogenized catalog). The observed annual rates considering magnitudes 4.0–6.0 in the surrogate catalog suggest a $b$-value of 0.9. For higher magnitudes the observed rates are more scattered (Fig. 11), but they still fall within the modeled recurrence rates taking into account the uncertainty on the $b$-value (Weichert, 1980). High magnitude rates are expected not to line up, as the recurrence times of such events are long with respect to the observation time window. As for the earthquake catalog homogenized in magnitude, the observed rates fall on a linear segment on the magnitude interval 4.25–6.0 (again with a slope close to 0.9–1). Applying the magnitude conversion on $m_b$ and $M_D$ magnitudes produces an increase of rates for all magnitudes up to 5.5. For both catalogs, there are many more events with magnitudes 3.5–4.0 than expected if one extrapolates the recurrence curves modeled on $M$4+ down to these magnitude intervals. This is a feature that we have observed in all catalogs, varying the degree of the declustering and/or removing zones characterized by dense swarms (such as the Pisayambo zone; Troncoso, 2009). For now, we have no clear explanation for this observation.

Comparing the recurrence curves obtained from both catalogs, the impact of the decision on the homogenization of magnitudes proves to be noticeable up to magnitudes 5.5–6. From magnitudes ≥6, the rates are quite similar. The average rate, for an earthquake with a magnitude ≥6.0 inside the spatial zone considered, varies between 0.05 and 0.1, resulting in an average recurrence time within 10 and 20 years (Fig. 12). As the clustered events have been excluded from the catalog, the recurrence curve describes the frequencies of Poissonian independent events. A recurrence time of 20 years leads to an ∼37% probability of not observing such an earthquake in the next 20 years in the area, or an ∼18% probability of observing two such events in the same future time window (Fig. 12; see also Beauval *et al.*, 2008).

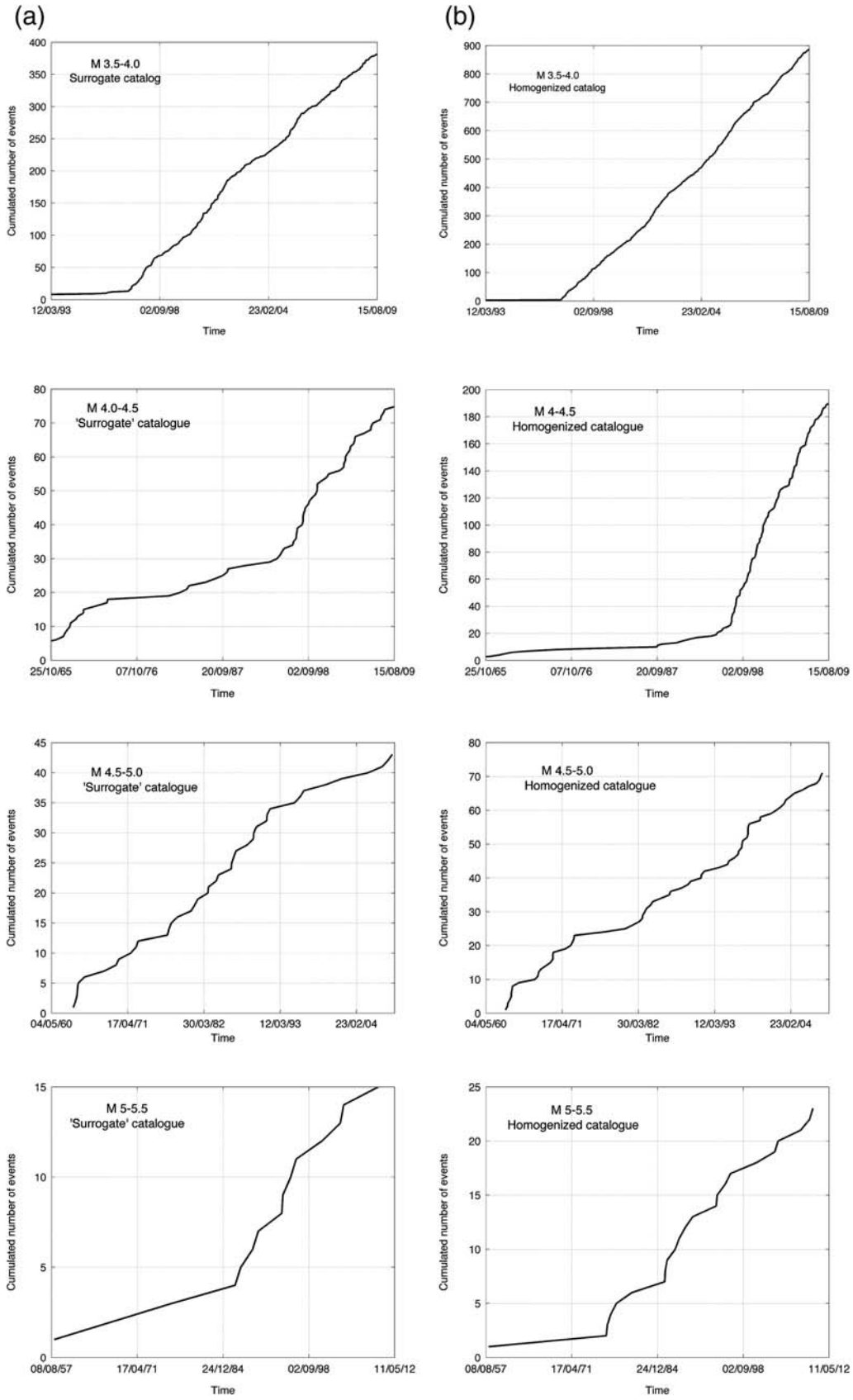


**Figure 8.** Cumulated number of events versus time, for different magnitude intervals, based on the declustered catalog enclosed in the spatial window focused on the Cordillera (Fig. 7): longitude −79.5° to −77.25°, latitude −2.5° to +1°, down to 40 km. (a) Plots based on the "surrogate" catalog (no conversion of magnitudes). (b) Plots based on the catalog homogenized in magnitude.

Table 6
Completeness Time Windows Valid for the Cordillera Region
(Longitudes −79.5° to −77.25° and Latitudes −2.5° to 1°)

| Magnitude Interval | [3.5–4.[ | [4.–4.5[ | [4.5–5.[ | [5.–5.5[ | [5.5–6[ | [6.–6.5[ | [6.5–7.[ | [7.–7.5[ |
|---|---|---|---|---|---|---|---|---|
| Time period of completeness | 1997 | 1997 | 1963 | 1957 | 1920 | 1860 | 1860 | 1587 |

## Conclusions

The earthquake catalog is ready for use in seismic hazard studies in Ecuador. Standard techniques and well-established criteria are applied to merge different instrumental sources and select the best earthquake solutions among existing ones. This catalog is intended to evolve as new information emerges, and some solutions will need updating. The historical part is appended to the instrumental unified catalog. Thirteen historical events are analyzed so that magnitudes (equivalent to $M_w$) and locations can be assigned for these events. They complete the initial historical data set published in Beauval *et al.* (2010), made of well-described historical earthquakes. Until more data is available with an intrinsic $M_w$, we believe that the uncertainty on the magnitude must be taken into account. Therefore, the earthquake catalog includes both the original magnitudes (calculated on waveforms) and $M_w$ obtained through conversion equations, and we recommend that users do calculations with both options.

The catalog is much more complete in the Cordillera region than on the coast. At least one historical earthquake of the nineteenth century (3 May 1896), that might be a subduction event, still needs to be analyzed. In the absence of more written documents, however, the length of the earthquake history along the coast will remain short (from the end of the nineteenth century on). For estimating the recurrence of large subduction events, other types of information are needed, such as geodetic measurements (ongoing work in Ecuador) and paleoseismic techniques (trenching for tsunamigenic deposit analyses or coral dating). For the Cordillera region, between latitudes −2.5° and +1°, the 500 years of data enable us to derive a recurrence curve for crustal earthquakes with magnitudes 4.0 and above, predicting on average an earthquake with magnitude $M_w \geq 6.0$ every 10–20 years. This result includes the uncertainty on the homogenization of magnitudes, as well as an uncertainty on the declustering step.

This work is part of a broader program aimed at estimating probabilistic seismic hazard at the level of the country. Others are currently working on the seismotectonic zoning, using knowledge of active tectonics, and taking advantage of this new unified earthquake catalog (Alvarado, 2012). The next step is the building of frequency–magnitude distributions for each source zone of this zoning. These distributions will be key inputs for the calculation of probabilistic seismic hazard maps. Where possible, the distributions will be combined with geodetic analysis and paleoseismology results (currently only the Pallatanga fault system has been analyzed using paleoseismology; S. Baize *et al.*, unpublished manuscript, 2012).

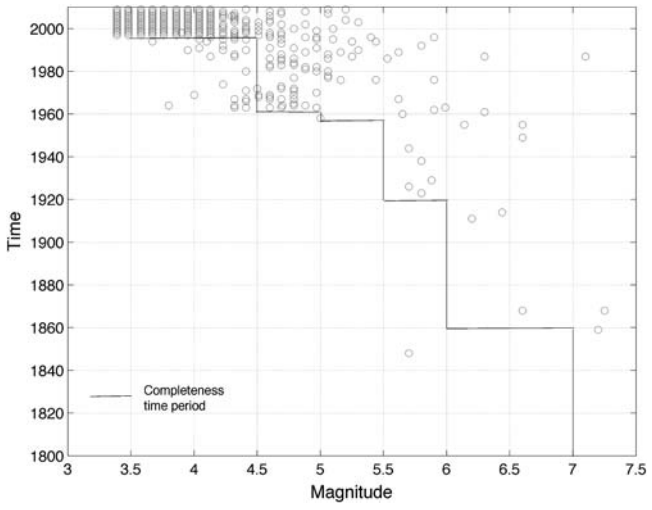


**Figure 9.** Declustered and homogenized catalog in the Cordillera: distribution of crustal earthquakes in time and magnitude, spatial window: longitude −79.5° to −77.25°, latitude −2.5° to +1°. Completeness time windows are indicated, see Table 6.

## Data and Resources

International Seismological Centre online bulletin, http://www.isc.ac.uk/iscbulletin/search/bulletin/ (last accessed November 2012). GCMT earthquake catalog, http://www

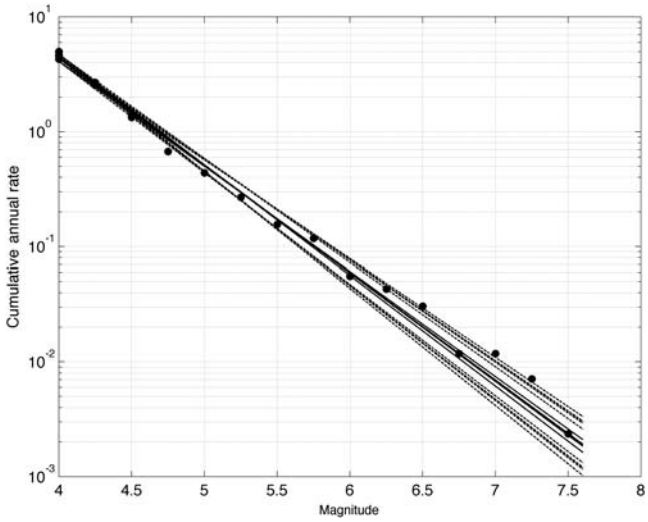


**Figure 10.** Implications of the declustering on the modeling of the Gutenberg–Richter curve, based on the surrogate earthquake catalog. Five sets of parameters in Reasenberg's (1985) algorithm are tested (Table 5). Observed rates plus parameters *a* and *b* are calculated five times and superimposed.

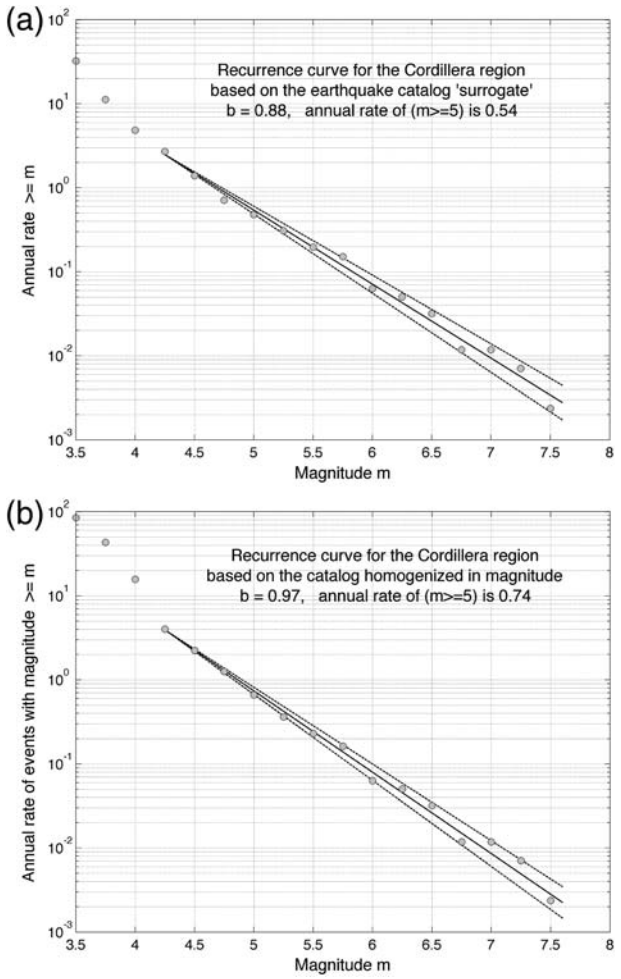


**Figure 11.** Recurrence curve for the Cordillera region (spatial window: longitude −79.5° to −77.25°, latitude −2.5° to +1°), calculated using the completeness time windows per magnitude interval. Observed seismicity rates (cumulated), gray circles. Recurrence curve taking into account the uncertainty on the *b*-value, dashed lines. The earthquakes are taken into account down to 40-km depth. The maximum magnitude for this zone is 7.6 (1797). (a) Surrogate catalog. (b) Homogenized catalog.

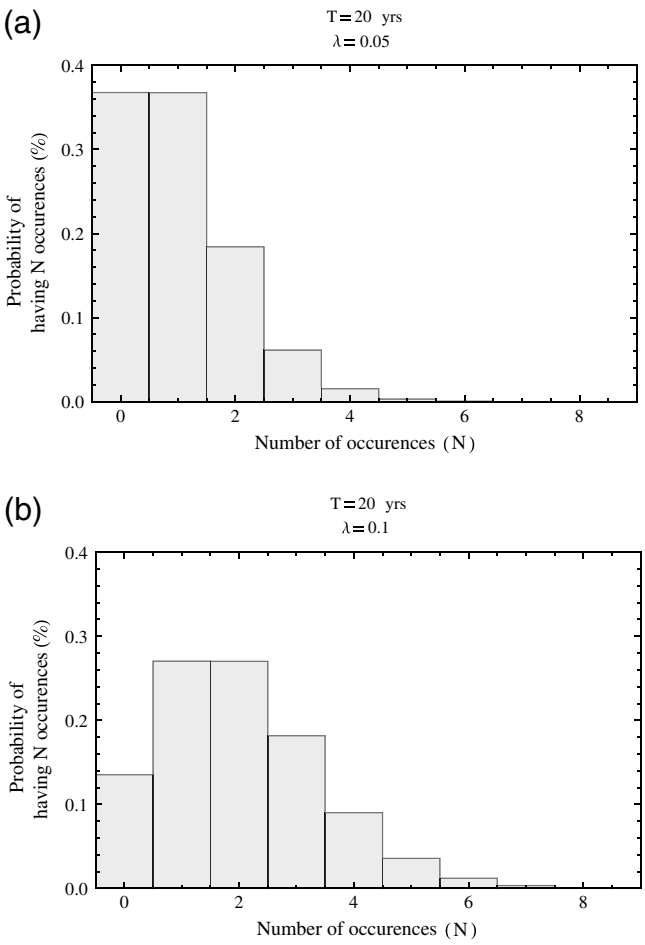


**Figure 12.** Expected number of earthquakes with magnitude ≥ 6.0, in a 20-yr time window, within the Cordillera zone considered (spatial window: longitude −79.5° to −77.25°, latitude −2.5° to +1°). (a) Poisson process with annual rate 0.05 (recurrence time 20 yr). (b) Poisson process with annual rate 0.1 (recurrence time 10 yr).

.globalcmt.org/CMTsearch.html (last accessed November 2012). PDE-NEIC earthquake catalog, http://earthquake.usgs.gov/earthquakes/eqarchives/epic/ (last accessed November 2012). Centennial catalog, http://earthquake.usgs.gov/research/data/centennial.php (last accessed November 2012). Code cluster 2000 (Reasenberg, 1985), http://earthquake.usgs.gov/research/software/index.php (last accessed November 2012).

## Acknowledgments

This work was partially supported by the laboratory ISTerre, by the Agence Nationale de la Recherche through the project Andes du Nord (Contract Number ANR-07-BLAN-143) and by IRD (Institut de la Recherche pour le Développement). On the Ecuadorian side, partial support was available from the Secretaría Nacional de Educación Superior, Ciencia y Tecnología SENESCYT (Proyecto PIN_08-EPNGEO-00001). This work was finalized within the recently created IRD joint international laboratory between France and Ecuador, LMI "Séismes et Volcans". We are grateful to F. Hollender for his kind help in drawing the second figure of the manuscript.

## References

Abe, K. (1981). Magnitudes of large shallow earthquakes from 1904 to 1980, *Phys. Earth Planet. In.* **27,** 72–92.

Abe, K. (1984). Complements to "Magnitudes of large shallow earthquakes from 1904 to 1980", *Phys. Earth Planet. In.* **34,** 17–23.

Alvarado, A. (2012). Néotectonique et cinématique de la déformation continentale en Equateur, *Thèse de doctorat (PhD)*, Université de Grenoble, France, 259 pp.

Bakun, W. H., and C. M. Wentworth (1997). Estimating earthquake location and magnitude from seismic intensity data, *Bull. Seismol. Soc. Am.* **87,** 1502–1521.

Beauval, C., and O. Scotti (2003). Mapping b-values in France using two different magnitude ranges: Possible non power-law behavior, *Geophys. Res. Lett.* **30,** no. 17, 1892, doi: 10.1029/2003GL017576.

Beauval, C., and O. Scotti (2004). Quantifying sensitivities of Probabilistic Seismic Hazard Assessment for France to earthquake catalog uncertainties, truncation of ground-motion variability and magnitude limits, *Bull. Seismol. Soc. Am.* **94,** 1579–1594.

Beauval, C., P.-Y. Bard, S. Hainzl, and P. Guéguen (2008). Can strong motion observations be used to constrain probabilistic seismic hazard estimates? *Bull. Seismol. Soc. Am.* **98,** 509–520.

Beauval, C., H. Yepes, W. H. Bakun, J. Egred, A. Alvarado, and J.-C. Singaucho (2010). Locations and magnitudes of historical earthquakes in the Sierra of Ecuador (1587–1996), *Geophys. J. Int.* **181,** 1613–1633, doi: 10.1111/j.1365-246X.2010.04569.x.

Braunmiller, J., N. Deichmann, D. Giardini, S. Wiemer, and the SED Magnitude Working Group (2005). Homogeneous moment-magnitude calibration in Switzerland, *Bull. Seismol. Soc. Am.* **95,** no. 1, 58–74.

Christophersen, A., and E. G. C. Smith (2008). Foreshock rates from aftershock abundance, *Bull. Seismol. Soc. Am.* **98,** no. 5, 2133–2148.

Christophersen, A., M. C. Gerstenberger, D. A. Rhoades, and M. W. Stirling (2011). Quantifying the effect of declustering on probabilistic seismic hazard, in *Proc. of the Ninth Pacific Conf. on Earthquake Engineering: Building an Earthquake-Resilient Society*, Auckland, New Zealand, 14–16 April, 8 pp.

Dimate, C., L. Drake, H. Yepez, L. Ocola, H. Rendon, G. Grünthal, and D. Giardini (1999). Seismic hazard assessment in the Northern Andes (PILOTO project), *Ann. Geofisc.* **42,** no. 6, 1039–1055.

Egred, J. (2009). Catalogo de Terremotos del Ecuador 1541–2009, Escuela Politecnica Nacional, Instituto Geofisico, internal report.

Ekström, G., M. Nettles, and A. M. Dziewonski (2012). The global CMT project 2004–2010: Centroid-moment tensors for 13,017 earthquakes, *Phys. Earth Planet. In.* **200–201,** 1–9.

Engdahl, E. R., and A. Villaseñor (2002). Global Seismicity: 1900–1999, in *International Handbook of Earthquake and Engineering Seismology*, Part A, Chapter 41, W. H. K. Lee, H. Kanamori, P. C. Jennings, and C. Kisslinger (Editors), Academic Press, 665–690.

Engdahl, E. R., R. Van Der Hilst, and R. Buland (1998). Global teleseismic earthquake relocation with improved travel times and procedures for depth determination, *Bull. Seismol. Soc. Am.* **88,** 722–743.

Font, Y., S. Segovia, S. Vaca, and T. Theunissen (2013). Seismicity pattern along the Ecuadorian subduction zone: New constrains from earthquake location in a 3D a priori velocity model, *Geophys. J. Int.* (in press).

Giesecke, A., A. A. Gomèz Capera, I. Leschiutta, E. Migliorini, and L. R. Valverde (2004). The CERESIS earthquake catalog and database of the Andean Region background, characteristics and example of use, *Ann. Geophys.* **47,** 421–435.

Grunewald, E. D., and R. S. Stein (2006). A new 1649–1884 catalog of destructive earthquakes near Tokyo and implications for the long-term seismic process, *J. Geophys. Res.* **111,** B12306.

Grünthal, G. (Editor) (1998). European Macroseismic Scale 1998 (EMS-98), *Cahiers du Centre Européen de Géodynamique et de Séismologie 15*, Centre Européen de Géodynamique et de Séismologie, Luxembourg, 99 pp.

Gutenberg, B., and C. F. Richter (1954). *Seismicity of the Earth and Associated Phenomena*, Princeton University Press, Princeton, New Jersey.

International Seismological Centre (2010). *EHB Bulletin*, Internatl. Seis. Cent., Thatcham, United Kingdom, http://www.isc.ac.uk (last accessed November 2012).

Johnston, A. C., and S. Halchuk (1993). The seismicity database for the Global Seismic Hazard Assessment Program, *Ann. Geofisc.* **3–4,** 133–151.

Lolli, B., and P. Gasperini (2003). Aftershocks hazard in Italy. Part I: Estimation of time-magnitude distribution model parameters and computation of probabilities of occurrence, *J. Seismol.* **7,** 235–257.

Mendoza, C., and J. W. Dewey (1984). Seismicity associated with the Great Colombia-Ecuador earthquake of 1942, 1958, and 1979: Implications for barrier models of earthquake rupture, *Bull. Seismol. Soc. Am.* **74,** 577–593.

Pacheco, J. F., and L. R. Sykes (1992). Seismic moment catalog of large shallow earthquakes, 1900 to 1989, *Bull. Seismol. Soc. Am.* **82,** 1306–1349.

Palacios, P., and H. Yepes (2011). Analysis de la magnitud de duracion, Instituto Geofisico, Escuela Politecnica Nacional, Quito, internal report, 18 pp (in Spanish, available on request).

Reasenberg, P. A. (1985). Second-order moment of central California seismicity, *J. Geophys. Res.* **90,** 5479–5495.

Rothé, J. P. (1969). *The Seismicity of the Earth, 1953–1965*, UNESCO, Paris.

Scordilis, E. M. (2006). Empirical global relations converting $M_S$ and $m_b$ to moment magnitude, *J. Seismol.* **10,** 225–236.

Segovia, M., and A. Alvarado (2009). Breve análisis de la sismicidad y del campo de esfuerzos en el Ecuador, in *Geología y geofísica marina y terrestre del Ecuador: desde la costa continental hasta las Islas Galápagos*, J.-Y. Collot, V. Sallares, and N. Pazmiño (Editors), Guayaquil-Ecuador, 131–150.

Swenson, J. L., and S. L. Beck (1996). Historical 1942 Ecuador and 1942 Peru subduction earthquakes, and earthquake cycles along Colombia–Ecuador and Peru subduction segments, *Pure Appl. Geophys.* **146,** 67–101.

Troncoso, L. (2009). *Estudio sismologico del Nido de Pisayambo, Memoria Master 2*, Université Nice Sophia-Antipolis, France, 26 pp.

Utsu, T. (2002). Relationships between magnitude scales, in *International Handbook of Earthquake and Engineering Seismology*, Part A, Chapter 44, W. H. K. Lee, H. Kanamori, P. C. Jennings, and C. Kisslinger (Editors), Academic Press, 733–746.

Weichert, D. H. (1980). Estimation of the earthquake recurrence parameters for unequal observation periods for different magnitudes, *Bull. Seismol. Soc. Am.* **70,** no. 4, 1337–1346.

Yadav, R. B. S., P. Bormann, B. K. Rastogi, M. C. Das, and S. Chopra (2010). A homogeneous and complete earthquake catalog for Northeast India and the Adjoining region, *Seismol. Res. Lett.* **80,** no. 4, 609–627.

ISTerre
IRD-CNRS-UJF
BP 53, 38041 Grenoble Cedex 9
France
celine.beauval@ujf-grenoble.fr
(C.B.)

Instituto Geofísico,
Escuela Politécnica Nacional
Ladrón de Guevara E11-253, Aptdo 2759
Quito, Ecuador
(H.Y., P.P., M.S., A.A., L.T., S.V., J.A.)

Géoazur
IRD-CNRS-UNS-OCA
250 rue Albert Einstein
Sophia-Antipolis 06560 Valbonne
France
(Y.F.)

Pontificia Universidad Católica del Ecuador
Av. 12 de Octubre y Patria
Quito, Ecuador
(J.A.)

Manuscript received 30 August 2012